Rotational spectra and structures of small clusters: The Ar4–H/DF pentamers

ARTICLE *in* THE JOURNAL OF CHEMICAL PHYSICS · FEBRUARY 1988

Impact Factor: 2.95 · DOI: 10.1063/1.453984

Rotational spectra and structures of small clusters: The Ar_4–H/DF pentamers

H. S. Gutowsky, Carl Chuang, T. D. Klots, Tryggvi Emilsson, R. S. Ruoff, and Karl R. Krause

Noyes Chemical Laboratory, University of Illinois, Illinois 61801

(Received 12 October 1987; accepted 16 November 1987)

The $^{40}Ar_4$–HF and –DF clusters have been identified and characterized by their microwave rotational spectra using a Flygare–Balle FT spectrometer with a pulsed supersonic nozzle to generate and detect the clusters. The observed $J = 2 \rightarrow 3$ to $6 \rightarrow 7$ transitions have fine structure limited to $K = 0, \pm 3$ and ± 6, indicative of symmetric tops with a threefold axis of symmetry produced by $I = 0$ nuclei. For Ar_4–HF the rotational constants B_0, D_J, and D_{JK} are 623.4539(1) MHz, 1.062(1) kHz, and 0.611(31) kHz, respectively; and for Ar_4–DF, 618.5846(1) MHz, 1.030(1) kHz, and 0.665(4) kHz. The results show that the clusters consist of the trigonal Ar_3–H/DF tetramer reported earlier, with a fourth argon on the back side of the Ar_3 group to form a tetrahedral or near tetrahedral Ar_4. In both clusters the H/DF lies along the threefold axis of the Ar_3 group, with the H/D end pointed at its face. If one assumes an Ar–Ar distance of 3.85 Å for both clusters, the Ar_3 plane to HF c.m. distance for Ar_4–HF with a tetrahedral Ar_4 is 2.713 Å compared to 2.735 Å for Ar_3–HF. The nuclear hyperfine structure of the rotational transitions shows that the H/DF experiences large amplitude bending vibrations with respect to the C_3 symmetry axis. The average amplitude for HF (40.4°) is comparable with that reported for the smaller Ar_m–HF complexes ($m = 1, 2, 3$). However, for DF the apparent 25.1 (1.6)° amplitude found is 10° less than that in the smaller complexes. The difference is attributed to an increased electric field gradient at the D in the pentamer. A possibly related feature is an Ar_4 c.m. to F distance which is 0.013 Å *longer* for Ar_4–DF than for Ar_4–HF.

INTRODUCTION

In previous studies of the argon/HF system, rotational spectra for the ground vibrational state were observed for a number of weakly bound species including the Ar_m–H/DF series with $m = 1,2,3$. They are formed in the supersonic expansion of argon seeded with H/DF. The first to be characterized was the Ar–HF dimer, in experiments with the molecular beam electric resonance method.[1] The Ar–DF counterpart was studied later,[2] including observations made with a Flygare–Balle Fourier transform microwave spectrometer.[3] The dimer is linear, with the H/D between Ar and F, and the HF/DF making large amplitude bending vibrations about the a axis (41.6° for HF and 33.5° for DF).

Our group extended the studies of the dimer to the Ar_2–H/DF[4] and Ar_3–H/DF[5] clusters with the Mark II Flygare–Balle spectrometer[6] aided by several improvements in its sensitivity.[5] The trimer is a T-shaped asymmetric top with C_{2v} symmetry while the tetramer is an oblate symmetric top with a threefold symmetry axis generated by an equilateral Ar_3. In both clusters the H/D is attracted equally by the argon atoms in the Ar_m, and the HF has a vibrational amplitude of ~41° with respect to the figure axis. The dimensions and internal dynamics of the two clusters are comparable with those found for the Ar–HF[1-3] and Ar_2[7] dimers. Similar results have been obtained for the Ar_m–HCl clusters ($m = 1,2,3$).[8]

Earlier efforts to continue the Ar_m–H/DF series through the pentamer were unsuccessful.[5] However, the signal acquisition and averaging capabilities of the spectrometer were improved recently,[9] enabling us to detect the rotational spectra of Ar_4–H/DF pentamers and determine their structures. They are trigonal symmetric tops like Ar_3–H/DF but with an argon on the figure axis at the backside of the Ar_3 to form a tetrahedral or near tetrahedral Ar_4 (Fig. 1). The details of the study are reported herein.

EXPERIMENTAL

Except for the signal digitizing and averaging system the spectrometer and experimental procedures were pretty much as described for the Ar_3–H/DF work.[5] A microwave pulse is applied to an evacuated Fabry–Perot cavity tuned to the microwave frequency, synchronized with a pulsed, supersonic jet of a gas mixture. The expansion cools the gas and generates the clusters. If the microwave frequency is within

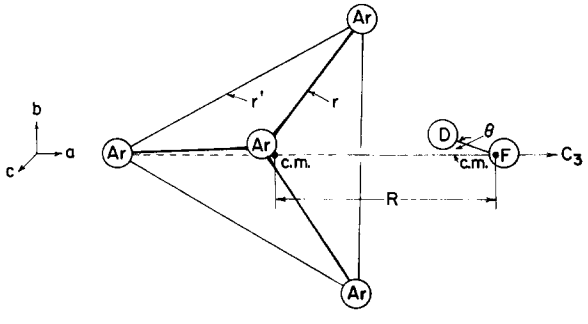

FIG. 1. Geometrical structure and inertial axes of the Ar_4–DF cluster. The atomic positions in the prolate symmetric top are drawn to scale; θ is the "average" angle between the figure (a) axis and the DF axis.

 0021-9606/88/052919-06$02.10

~0.5 MHz of a rotational transition, a free induction decay (FID) of its rotational polarization appears in the cavity after the microwave pulse itself has decayed. The FID is detected, digitized, and averaged for a number of microwave and gas pulses, then Fourier transformed to give a frequency spectrum as shown in Fig. 2, which gives a couple of examples of the hyperfine structure (hfs) selected for their better S/N.

The main functional improvement made recently is the ability to apply multiple microwave pulses and record their FIDs without dead time. Moreover, the signal averaging occurs while the trailing edge of a gas pulse is exiting the cavity. The digitizer has 4096 words of memory and the number of points (words) per FID is adjustable. Experience has shown that FIDs taken at any time during the first ~1 msec after the gas pulse look much the same. Current practice in searches is to use 256 points/FID and apply 16 MW pulses/gas pulse. A controller clocks and sequences the 4096 points from the individual FIDs and, when a series is complete, sends them to an IBM prototype card for averaging by hardware on the card. A similar series is run while the gas pulse is off and subtracted to reduce noise. The CPU has direct access to memory for averaging which, therefore, is very fast so that 12 gas pulses can be processed per second. When transforms are desired, the number of points/FID is doubled (to 512) to improve resolution.

Argon and also first run neon (Airco), which consists of 70% neon and 30% helium, were used as the carrier gas at ambient temperature. We have found that use of first run neon usually improves the S/N several-fold over pure argon as the carrier gas for Ar_m–HF and –HCl clusters. For it the optimum conditions were a backing pressure of ~1.7 atm with ~20% argon and 0.03% of a 50–50 mixture of HF and DF. The HF was from Linde; the DF was synthesized locally by reaction of D_2 with F_2. With argon as the carrier, the backing pressure was 0.5 atm and the H/DF was ~0.1%. It was noted that the lines liked very little HF or DF for best signal. In some experiments resolution was improved by suppressing the Doppler broadening with a Laval type nozzle and adjustable skimmer.[5]

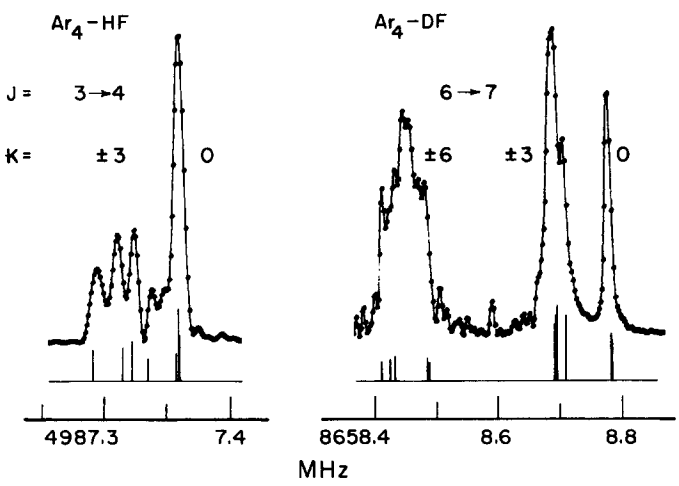

FIG. 2. Centrifugal distortion and hyperfine structure of the $J = 3 \rightarrow 4$ and $J = 6 \rightarrow 7$ transitions of Ar_4–HF and Ar_4–DF, respectively. The $J = 3 \rightarrow 4$ spectrum (left) was obtained in 10 min by averaging 60 000 FID's digitized at 200 ns for 512 points, giving a transform with resolution of 1.22 kHz/point when zero-filled three times. The $J = 6 \rightarrow 7$ spectrum (right) took 60 min for 315 000 FID's; the transform was zero-filled twice, giving a resolution of 1.44 kHz/point. The Doppler doubling has been suppressed. The stick spectra (bottom) were calculated with the rotational parameters given in Table III. The scale for Ar_4–DF is half that for Ar_4–HF.

RESULTS AND ANALYSIS

Search and assignment

Several searches were made for the Ar_4–HF pentamer over a period of more than two years. The most likely structure for it was considered to be the symmetric top obtained by adding a fourth Ar to the backside of Ar_3–HF to form a tetrahedral or near-tetrahedral Ar_4. This approach predicts a B_0 rotational constant of 621 MHz which compares favorably with the value of 623.5 MHz actually found. The earlier searches were unsuccessful primarily because of inadequate sensitivity. In them a weak single line was noted at 4987.363 MHz, which we now know is the $K = 0, J = 3 \rightarrow 4$ transition of Ar_4–HF. However, the nearby $K = \pm 3$ transition with its readily identified, symmetric-top hfs (Fig. 2) was too weak for detection.

Instead, serendipity led us recently to the $K = 0$, $J = 2 \rightarrow 3$ transitions of the Ar_4–HF and –DF pentamers in a search being made for an a dipole, $J = 0 \rightarrow 1$ transition of an (HFDF)–Ar trimer. A 50–50 mixture of HF and DF was being used in the search, our first application of the new data acquisition system described in the Experimental section. In it, observation of a weak line at 3711 MHz was followed by another equally weak line at 3740 MHz, both without resolved hfs. At that point they were recognized as probably $K = 0$ transitions from the Ar_4–H/DF symmetric tops. The lines disappeared when first run neon was used as the carrier gas but returned when argon was added to the mixture, indicating the presence of argon in the species being observed. Similarly the presence of DF and HF in the species responsible, respectively, for the low and high frequency lines was established by the dependence of their relative intensities upon the HF/DF ratio in the carrier gas.

Assignment of the species as Ar_4–H/DF symmetric tops was confirmed by observation at higher frequencies, as given in Table I, of two series of nearly equally spaced sets of lines, each described by the following expression for the $J \rightarrow J + 1$, $\Delta K = 0$ transitions of a symmetric top[10]:

$$\nu_0 = 2B_0(J+1) - 4D_J(J+1)^3 - 2D_{JK}(J+1)K^2. \quad (1)$$

Many of the transitions exhibit nuclear hfs as well as the splittings associated with the K-dependent centrifugal distortion term in D_{JK}. Their analysis is very similar to that described in more detail for Ar_3–H/DF[5] and Ar_3–HCl.[8]

The splittings produced by D_{JK} were found only for K's which are an integral multiple of three. Thus, neglecting the hfs for the moment, for a given $J \rightarrow J + 1$ transition when $J \leqslant 2$, there is no splitting, when $3 \leqslant J \leqslant 5$ there is a pair of lines, and when $6 \leqslant J \leqslant 8$ there are three lines. This type of behavior was also found for Ar_3–H/DF.[5] It occurs for symmetric tops with a three-fold symmetry axis which interchanges

TABLE I. Fitting of the line centers for the rotational transitions of the Ar_4–HF and Ar_4–DF clusters.[a]

	Ar_4–HF		Ar_4–DF	
$J,K \rightarrow J+1,K$	Obs. (MHz)	Diff. (kHz)	Obs. (MHz)	Diff. (kHz)
2,0→3,0	3740.6090	0.2	3711.3966[b]	−0.1
3,0→4,0	4987.3590	−0.5	4948.4133	−0.3
±3→±3	7.315[b]	[d]	8.3667[b]	1.0
4,0→5,0	6234.0086	0.5	6185.3320	0.3
±3→±3	3.950[c]		5.2718[b]	0
5,0→6,0	7480.5292	−0.1	7422.1263	0.1
±3→±3	0.462[c]		2.0542[b]	−0.2
6,0→7,0			8658.7724	−0.1
±3→±3			8.6882[b]	−0.5
±6→±6			8.450[c]	

[a] Transition frequencies observed for states with $K \neq 0$ are emphasized by omitting the first three digits, which are the same as for the transition just above.
[b] Determined by fitting of hfs.
[c] Approximate line center of partially resolved hfs; not used in the fit.
[d] Fitted exactly by choice of D_{JK}.

identical $I = 0$ nuclei, in the present case the three off-axis ^{40}Ar nuclei (Fig. 1). The presence on the C_3 axis of a fourth argon is indicated by the small B_0 value, a point considered in more detail in the inertial analysis.

Hyperfine structure and rotational constant

The hyperfine structure of Ar_4–HF is produced by the vibrationally averaged projection D_a of the H–F magnetic dipole–dipole interaction on the a-inertial axis of the cluster, and that in the DF cluster by the deuterium quadrupole interaction χ_a plus the D–F dipole–dipole interaction. We make the usual assumption that the structure of free H/DF is unchanged in the cluster, in which case χ_a is given by

$$\chi_a = (\chi_0/2)\langle 3\cos^2\theta - 1\rangle, \quad (2)$$

and D_a (HF or DF) by a similar equation. χ_0 and D_0 are the interaction constants in free H/DF,[11] and θ is the angle between the H/DF and the a axis. The same basis functions and procedures were used to calculate the hfs as for Ar_3–H/DF.[5] Spin-rotation was neglected and matrix elements of the Hamiltonian were determined by applying tensor methods to the basis set

$$I_{H/D} + I_F = I,\ I + J = F. \quad (3)$$

The hfs was fitted individually for each K, with the line center and χ_a and/or D_a as adjustable parameters.

In Ar_4–HF the four $K = 0$ transitions (observed for $J = 2\rightarrow3$ to $5\rightarrow6$) are single lines with a full width at half-height of about 10 kHz, shown by calculation to consist of unresolved hfs. For them, the line center was taken to be the frequency of maximum intensity (Table I). Their fit with Eq. (1) gave a B_0 of 623.4539(1) MHz and a D_J of 1.062(1) kHz. The hfs for the $K = \pm 3, J = 3\rightarrow4$ transition is a set of four well resolved components (Fig. 2). It was fitted to determine the line center and D_a (HF). Inclusion of the spin-rotation interaction had a negligible effect on the fit; we report our results without it. The value of D_{JK} was determined from the line centers for the $K = 0$ and $\pm 3, J = 3\rightarrow4$ transitions. The various results are given in Tables I–III including a value for the average, HF-bending angle θ obtained via Eq. (2) from D_a (HF). The $K = \pm 3, J = 4\rightarrow5$ and $5\rightarrow6$ transitions were not used in the fitting. They have a single peak with an unresolved shoulder. Their line shapes and frequencies are consistent with those predicted from the fitted constants.

The results for Ar_4–DF and their analysis are quite similar to these for the HF containing cluster. Five $K = 0$ transitions were observed. That for $J = 2\rightarrow3$ at 3711.397 MHz was resolved into two components, one a weak shoulder separated by 14.3 kHz from the main line. They were fitted with the line center as an adjustable parameter and X_a (D) and D_a (DF) as another, the latter two combined by their mutual dependence on θ (Table II). The other four $K = 0$ transitions were single, symmetrical lines. The five line centers (Table I) were fitted by Eq. (1) to obtain B_0 and D_J (Table III).

The $K = \pm 3$ transitions of Ar_4–DF were observed for $J = 3\rightarrow4$ to $6\rightarrow7$. That for J = 3→4 is an unresolved bunch of lines about 30 to 40 kHz wide with a single peak at higher frequencies on top of the K = 0 transition. For $J = 4\rightarrow5$ to $6\rightarrow7$ the $K = \pm 3$ transitions were resolved into two peaks, the upper a weak shoulder separated from the main peak by 40.6, 25.5, and 15.7 kHz respectively. The observed hfs and the line centers and χ_a (D) values obtained by fitting it are given in Table II. The value of D_{JK} was found to be 0.665(4) kHz from the line centers for the $K = 0$ and $\pm 3, J = 5\rightarrow6$ and $6\rightarrow7$ transitions. The average value of χ_a (D) and the corresponding θ are listed in Table III. The $J = 4\rightarrow5$ data were not used because the components of the $K = \pm 3$ "doublet" are broad and weak.

Typical hfs and its fitting are shown in Fig. 2. Spectra observed for the $J = 3\rightarrow4$, $K = 0$ and ± 3 transitions of Ar_4–HF and for the $J = 6\rightarrow7$, $K = 0$, ± 3, and ± 6 transitions of Ar_4–DF are given, along with stick spectra calculated for these K's only. The $J = 6\rightarrow7$ results are included to demonstrate the C_3 symmetry of the symmetric top. The hfs for $K = \pm 6$ is too broad and weak for accurate analysis; however, its breadth of ~70 kHz is compatible with predictions based on the parameters determined by fitting the other transitions. The observed and calculated frequencies of the hfs are compared in Table II. In some instances the best fit is not as good as we'd like it to be; however, the discrepancies are attributable to poor S/N. For Ar_4–DF, treatment of χ_a (D) and the much smaller D_a (DF) as independent parameters did not improve the fits significantly; the results given are for them as a single parameter with $D_a \equiv (D_0/\chi_0)\chi_a$.

Inertial analysis

As usual with symmetric tops, there are more structural parameters to be evaluated than rotational constants available for the purpose. Even in the simplest case of a tetrahedral Ar_4, there are two distances to consider, the Ar–Ar distance r and the Ar_4 c.m. to H/DF c.m. distance R. However, one would expect the attraction between the H/DF and the three argons on the adjacent face (Fig. 1) to deform the tetrahedral Ar_4 slightly along the C_3 axis, so the Ar′–Ar distance r' is a little shorter or longer than the intrafacial r.

TABLE II. Observed and calculated frequencies of the hyperfine components in the $K = \pm 3$, $J = 3 \rightarrow 4$ transition of Ar_4–HF and the $K = 0$, $J = 2 \rightarrow 3$ and $K = \pm 3$, $J = 4 \rightarrow 5$ to $J = 6 \rightarrow 7$ transitions of Ar_4–DF.

Component		Obs.	Diff.	D_a/χ_a
J,I,F	$\rightarrow J',I',F'$	(MHz)	(kHz)	(kHz)
$K = \pm 3$, $J = 3 \rightarrow 4$ transition at 4987.315 MHz for HF species				
3,1,3	4,1,4	4987.293	2	52.9(66)
3,0,3	4,0,4	4987.310	−5	
3,1,4	4,1,5	4987.323	0	
3,1,2	4,1,3	4987.337	2	
$K = 0$, $J = 2 \rightarrow 3$ transition at 3711.397 MHz for DF species				
2,1/2,5/2	3,1/2,7/2	3711.394	1	246.6[a]
2,3/2,7/2	3,3/2,9/2		0	
2,3/2,5/2	3,3/2,7/2		−4	
2,3/2,5/2	3,1/2,5/2	3711.408	0	
$K = \pm 3$, $J = 4 \rightarrow 5$ transition at 6185.272 MHz for DF species				
4,1/2,7/2	5,1/2,9/2	6185.262	16	273.3
4,1/2,9/2	5,1/2,11/2		5	
4,3/2,11/2	5,3/2,13/2		−1	
4,3/2,9/2	5,3/2,11/2	6185.303	2	
4,3/2,7/2	5,3/2,9/2		−2	
$K = \pm 3$, $J = 5 \rightarrow 6$ transition at 7422.054 MHz for DF species				
5,1/2,9/2	6,1/2,11/2	7422.046	5	268.8
5,1/2,11/2	6,1/2,13/2		1	
5,3/2,7/2	6,3/2,9/2		0	
5,3/2,13/2	6,3/2,15/2		−3	
5,3/2,11/2	6,3/2,13/2	7422.072	1	
5,3/2,9/2	6,3/2,11/2		−1	
$K = \pm 3$, $J = 6 \rightarrow 7$ transition at 8658.688 MHz for DF species				
6,1/2,11/2	7,1/2,13/2	8658.683	2	260.5
6,1/2,13/2	7,1/2,15/2		1	
6,3/2,9/2	7,3/2,11/2		−1	
6,3/2,15/2	7,3/2,17/2		−2	
6,3/2,13/2	7,3/2,15/2	8658.699	0	
6,3/2,11/2	7,3/2,13/2		0	

[a] Uncertainties are not given for χ_a because only two components were resolved for $K = \pm 3$ and fitted exactly by the line center and χ_a.

TABLE III. Spectroscopic constants determined for the Ar_4–H/DF clusters.[a]

Isotopic species	B_0 (MHz)	D_J (kHz)	D_{JK} (kHz)	D_a/χ_a[b] (kHz)	θ (deg)
Ar_4–HF	623.4539(1)	1.062 (1)	0.611(31)	52.9(66)	40.4(1.8)
Ar_4–DF	618.5846(1)	1.0295(4)	0.665 (4)	259. (11)	25.1(1.6)

[a] Obtained by fitting the data in Tables I and II. Numbers in parentheses are the standard deviation of the last digit(s) in the fit.

[b] The value given for the HF species is D_a and that for DF is χ_a; D_a was also fitted for DF as an independent parameter, giving a less accurate value of θ.

There is also the question of which end of the H/DF is closest to the Ar_4. In the three smaller Ar_m–H/DF complexes it is the H/D end but the point should be checked in the present case. Finally, there are the effects of the large amplitude H/DF bending motion to consider.

If the Ar_4 in the cluster is tetrahedral, the moment of inertia I_B for the cluster is given by the parallel axis theorem to be

$$I_B = m_{Ar} r^2 + \tfrac{1}{2}(1 + \cos^2\theta) I_0(\text{H/DF}) + \mu_c R^2, \quad (4)$$

where $m_{Ar} r^2 = I_0(Ar_4)$ is the moment of inertia for the Ar_4 spherical top, I_0 (H/DF) is that for free HF or DF,[11] and μ_c is the reduced mass for the cluster treated as diatomic. In our calculations a conversion factor of 505 379.07 amu Å^2 was used for $I \times B$. The experimental values for I_B and θ in Table III convert Eq. (4) into a simple relationship between R and r. These functions are plotted in Fig. 3 for the Ar_4–HF and DF clusters for r's between 3.80 and 3.88 Å the central range of which corresponds to the values found for Ar_2–HX and Ar_3–HX (X = F,Cl).[4,5] The curves are nearly linear, that for Ar_4–DF (R') falling systematically ~0.032 Å below the one for Ar_4–HF (R).

With the reasonable assumption that H/DF substitution does not affect the structure of the Ar_4, the difference $\Delta R = R - R'$ between the two c.m. to c.m. distances is the sum of two contributions, the isotopic difference in the c.m. for HF and DF and any difference in the Ar_4 c.m. to F distance for HF vs DF. If we project the H/DF at their respective torsional angles onto a so that their fluorines are at the same position on a, the magnitude of the c.m. contribution to ΔR is found to be 0.0447 Å, positive if the H/D end is pointed at Ar_4 and negative if pointed away. For $r = 3.85$ Å the experimental value for ΔR in Fig. 3 is +0.0313 Å (3.4985 − 3.4672 Å). So we conclude that the H/D end is closest to the Ar_4, also that the Ar_4 c.m. to F distance is ~0.013 Å longer for the cluster with DF than with HF. This is comparable in magnitude with the results for the Ar–H/DF dimers except that the Ar–F distance in the dimer is 0.010 Å *shorter* for DF than for HF.[3]

A check on the consistency of our models for Ar_4– and Ar_3–H/DF can be made by comparing the Ar_3 plane to HF c.m. distances in them. For Ar_3–HF this corresponds to the Ar_3 c.m. to HF c.m. distance, which we found to be 2.735 Å with $r = 3.85$ Å.[5] In Ar_4–HF the Ar_4 c.m. to HF c.m. distance of 3.4985 Å includes the Ar_4 c.m. to Ar_3 plane distance. In a tetrahedral Ar_4 with $r = 3.85$ Å, this is $(2/3)^{1/2}$ $r/4 = 0.7859$ Å. Correcting for it, the Ar_3 plane to HF c.m. distance in the Ar_4–HF is 2.713 Å. The closeness of this value to the 2.735 Å for Ar_3–HF supports the basic features of our structural analyses. Also, it shows that any deviation

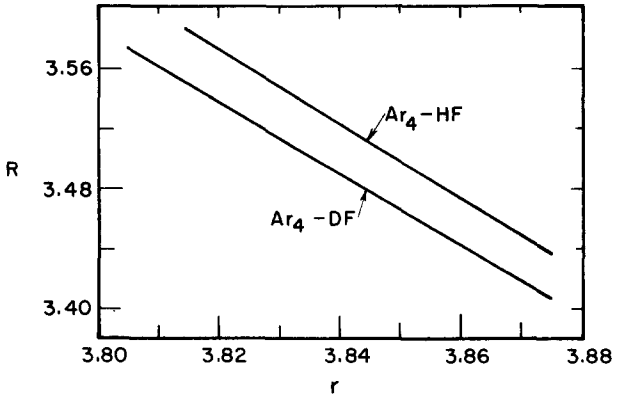

FIG. 3. A plot of interatomic distances (in Å) consistent with the B_0's and θ's observed for Ar_4–H/DF. R is the Ar_4 c.m. to H/DF c.m. distance and r is the Ar–Ar distance in an Ar_4 cluster assumed to be a rigid tetrahedron.

of the Ar_4 from tetrahedral is small. The results for the DF species are similar.

The rotational constant for the Ar_4–H/DF about its symmetry axis is virtually that of Ar_4; it also includes a small contribution from I_0(H/DF). With allowance for it the rotational constant about the symmetry axis is 852.9 MHz when $r = 3.85$ Å. Thus, the C_3 axis of Ar_4–H/DF is the a axis and the cluster is a prolate symmetric top.

DISCUSSION

In spite of the limited amount of quantitative structural information determinable from the rotational constants of symmetric tops, it is clear that the Ar-containing cluster we report here differs minimally from Ar_3–H/DF. For example, the structure of the $J = 3 \rightarrow 4$ transition reported for Ar_3–HF [Fig. 1 of Ref. 5(b)] is identical with that we attribute to Ar_4–HF in Fig. 2 of this report, except for the B_0 and D_{JK} values. Both symmetric tops have a threefold axis generated by $I = 0$ nuclei. The smaller B_0 of the present cluster, 623.5 MHz compared with 1188.2 MHz for Ar_3–HF, can be attributed reasonably only to addition of mass on the C_3 axis of the latter. Placing an Ar atom on the back side of the Ar_3–HF not only is the simplest way of doing this but also it fits B_0 with minimal change in the Ar–Ar and Ar_3 c.m. to HF c.m. distances (r and R) in the pentamer. Placement of a fourth Ar on the "front end" of Ar_3–HF to give an Ar_3–HF–Ar geometry would preserve the threefold axis. But this would surely change the HF bending amplitude. Moreover, to fit the B_0 observed for the pentamer, the HF c.m. to lone Ar distance would have to be 1.18 Å, which is impossibly short.

The small positive value of D_{JK} (0.611 kHz) found for the present species is also consistent with our identification of it as Ar_4–HF. In oblate symmetric tops D_{JK} is almost always negative and in prolate, positive.[12] For Ar_3–HX and Ar–Ar_3–HX symmetric tops, the rotational constant for rotation about the threefold symmetry axis is not experimentally available; however, it is determined by the dimensions of the Ar_3 group and should be ~ 850 MHz in all cases. In Ar_3–HF B_0 is 1188.2 MHz so 850 MHz $= C_0$, the top is oblate, and D_{JK} was found to be negative, -5.76 kHz.[5] For the present species, B_0 is 623.4 MHz, so 850 MHz $= A_0$, the top is prolate and D_{JK} should be positive, which agrees with the 0.611 kHz value found. Ar_3–HCl is a near spherical, prolate top with $B_0 = 843.9$ MHz, and in it $D_{JK} = 1.82$ kHz.[8]

An interesting feature of the present results is the apparent bending amplitude of 25.1° found for the DF species. In the Ar_m–HF series the amplitudes for $m = 1,2,3,$ *and* 4 are virtually identical: 41.6°, 40.7°, 41.0°, and 40.4°. For the DF counterparts there is what may be a slight trend to larger amplitudes for the lower three members: 33.5°, 35.0°, and 35.6°. For them the ratio of observed amplitudes θ_{HF}/θ_{DF} is close to the value $1.175 = (\mu_{DF}/\mu_{HF})^{1/4}$, as expected if the difference in amplitude is a purely mass effect. However, for Ar_4–H/DF the apparent ratio is 1.610, indicating the importance of another factor. The S/N for the transitions of Ar_4–DF leaves something to be desired, as may be seen in Fig. 2. Even so, our observations indicate quite strongly an apparent bending angle of about 25° rather than 35°. The breadth of the hfs is linear in $\frac{1}{2}\langle 3\cos^2\theta - 1\rangle$ and for 35° this factor is 2/3 what it is for 25°, a difference which cannot be bridged in the fitting process.

The most likely interpretation of the difference is that in the pentamer the field gradient at the deuterium is increased by its interaction with the argons, making χ_0(D) in the pentamer larger than in the free DF monomer. Such effects are usually small and difficult to separate from the vibrational averaging. The interactions in the rare gas–H/DX dimers are too weak for any sizable effects of this sort to have been reported for them.[3] However, we have recently found evidence for an appreciable increase of χ_o(D) for DCl in the Ar_3–DCl cluster.[13] If χ_o(D) and χ_o(Cl) are the same in a cluster as in free DCl, the apparent bending angles determined via Eq. (2) from χ_a(D) should be the same as from χ_a(Cl). But for Ar_3–$D^{35}Cl$, θ(D) is only 26.2° compared with 31.5° for $\theta(^{35}Cl)$, the difference most readily interpreted as an increase in χ_o(D). For the Ar–DCl dimer, θ(D) and $\theta(^{35}Cl)$ are more nearly alike, 31.6° and 33.8°, suggesting that the change in χ_o(D) increases with cluster size.

While a change in χ_o(D) is a plausible cause of the small apparent θ_{DF} in the Ar_4–DF pentamer, the origin of the change is a more difficult question. It seems that θ_{HF} and χ_o(D) are "normal" in Ar_3–H/DF and θ_{HF} in Ar_4–HF but χ_o(D) is "abnormal" in Ar_4–DF, implying that the potential surface (and field gradients) are quite similar for Ar_3–H/DF and Ar_4–HF but different for Ar_4–DF. A further indication of such a difference is our finding the Ar_4 c.m. to F distance to be ~ 0.013 Å *longer* for the cluster with DF than with HF although the two distances are about the same in the tetramers.[5] This suggests that in Ar_4–DF the radial and bending motions of the DF are coupled with those of Ar_4 in a manner differing from that of HF and from that in Ar_3–H/DF.

ACKNOWLEDGMENTS

Our work was supported by the National Science Foundation under Grants DMR-86-12860 and CHE-85-20519. Also, acknowledgment is made to the donors of The Petroleum Research Fund, administered by the American Chemical Society, for partial support of this research. We thank Cliff Dykstra for several helpful discussions of the potential surfaces for Ar_4–HF and Ar_3–HF.

[1] S. Harris, S. Novick, and W. Klemperer, J. Chem. Phys. **60**, 3208 (1974).
[2] T. A. Dixon, C. H. Joyner, F. A. Baiocchi, and W. Klemperer, J. Chem. Phys. **74**, 6539 (1981).
[3] M. R. Keenan, L. W. Buxton, E. J. Campbell, A. C. Legon, and W. H. Flygare, J. Chem. Phys. **74**, 2133 (1981).
[4] H. S. Gutowsky, T. D. Klots, C. Chuang, C. A. Schmuttenmaer, and T. Emilsson, J. Chem. Phys. **83**, 4817 (1985); **86**, 569 (1987).
[5] H. S. Gutowsky, T. D. Klots, C. Chuang, J. D. Keen, C. A. Schmuttenmaer, and T. Emilsson, J. Am. Chem. Soc. **107**, 7174 (1985); **109**, 5633 (1987).
[6] E. J. Campbell, W. G. Read, and J. A. Shea, Chem. Phys. Lett. **94**, 69 (1983), and earlier work cited therein.

[7]E. A. Colbourn and A. E. Douglas, J. Chem. Phys. **65**, 1741 (1976); see also H. F. Godfried and I. F. Silvera, Phys. Rev. Lett. **48**, 1337 (1982).
[8]T. D. Klots, R. S. Ruoff, C. Chuang, T. Emilsson, and H. S. Gutowsky, J. Chem. Phys. **87**, 4383 (1987).
[9]C. Chuang, T. Emilsson, and H. S. Gutowsky (to be published).
[10]C. H. Townes and A. L. Schawlow, *Microwave Spectroscopy* (McGraw–Hill, New York, 1955), pp. 48–82 and 149–173.
[11]J. A. Shea and W. H. Flygare, J. Chem. Phys. **76**, 4857 (1982), Table VI.
[12]W. Gordy and R. L. Cook, *Microwave Molecular Spectra*, 3rd ed., Techniques of Chemistry, Vol. XVIII (Wiley–Interscience, New York, 1984), Chap. 8.
[13]H. S. Gutowsky, R. S. Ruoff, and T. D. Klots (to be published.)